round-bottom flash equipped with a Dean-Stark condenser, and the solution was refluxed under a blanket of dry argon over a period of 16 h to remove the water of hydration from silver perchlorate. After the dehydration the benzene solution was cooled to room temperature followed by dropwise addition of a solution of triphenylsilyl chloride (3.13 g, 10.6 mmol) in 20 mL of dry benzene over a period of 5 min. The resulting mixture was stirred for 16 h at room temperature. After the reaction the benzene was evaporated under vacuum, the residue was extracted with 50 mL of dry dichloromethane, and the insoluble silver chloride was discarded. The dichloromethane extract on evaporation provided triphenylsilyl perchlorate as a gray powder, 2.5 g (66% yield). The material was further purified by recrystallization from a CH_2Cl_2/*n*-hexane solvent system and stored at 0 °C under dry argon.

Hydride-Transfer Experiments. To a suspension of 86 mg (0.25 mmol) of trityl perchlorate in 1.5 mL of dry dichloromethane in a flame-dried 10-mm NMR tube under a blanket of dry argon was added a solution of silane (0.25 mmol) in 1 mL of dry dichloromethane with vigorous stirring. A similar procedure was employed with other solvents. With the SO_2/SO_2ClF mixture the reaction was carried out at -78 °C. A similar mixing procedure was employed with SbF_5/SO_2ClF/trityl chloride as the hydride abstracting agent (-78 °C).

Preparation of $Me_2BrCSiBrMe_2$ (17). ^iPrMgBr in Et_2O, prepared by Grignard reaction of ^iPrBr (9 mL) and Mg turnings (2.7 g) was added dropwise to an ethereal solution of Me_2SiHCl (10.9 mL) at 0 °C, allowed to warm up to room temperature, and stirred for 1 h. The white finely powdered precipitate (MgBrCl) was filtered off, and the filtrate was distilled through a Vigreux column (<50 °C bath temperature) to remove the ether. The remaining solution was diluted with 10 mL of pentane and cooled to 0 °C. Bromine (2.5 g) in 5 mL of pentane was added dropwise whereby the bromine was immediately discolored. After the addition the pentane was distilled off, and the solution was kept at 60 °C while another 2.5 mL of bromine (neat) was introduced at such a rate as to maintain a slightly red solution. Toward the end of the addition the crude product started to precipitate and stick to the walls of the reaction flask. The crude solid was transferred into a sublimer, and after the sublimation pure product was obtained as a white waxlike material that fumed and turned brown when exposed to moist air. The overall yield was 55%. NMR: $\delta(^1H)$ 0.4 (Si-CH_3, 6 H), 1.5 (C-CH_3, 6 H); $\delta(^{13}C)$ -1 (Si-CH_3); 28 (C-CH_3); 53 (C-Br), $\delta(^{29}Si)$ 25.

Preparation of $Me_2BrSiSiBrMe_2$ (18). A suspension of 5 g of poly(dimethylsilane) in CCl_4 was cooled to -10 °C, and 3.6 g of bromine in 20 mL of CCL_4 was added dropwise over 2 h. The mixture was allowed to stand at room temperature for 1 h, and subsequently the solvent was evaporated under aspirator vacuum to yield 60% of the pure product (bp = 120 °C at 20 mmHg; mp = 40 °C). NMR: $\delta(^1H)$ 0.2; $\delta(^{13}C)$ 0.8; $\delta(^{29}Si)$ 12.

Note: The distillation jacket must be heated with steam or hot air to prevent clogging of the apparatus by the solid product.

Preparation of $Ph_2CBrSiBrMe_2$ (19). To 1.7 g of Ph_2CH_2 in 20 mL of dry THF was added dropwise 6.5 mL of *n*-BuLi (1.6 M in hexanes) at -78 °C, and the mixture was allowed to warm up to room temperature, whereupon the originally orange solution turned cherry red. Me_2SiHCl (1.1 mL) was then introduced at 0 °C, and the mixture was warmed up to room temperature and stirred overnight. After quenching with water, extraction with Et_2O (three times), and evaporation of the solvents, the remaining oil was slowly fractionated (Vigreux column) under reduced pressure, and the $Ph_2CHSiHMe_2$ fraction boiling at 80 °C (0.05 torr) was collected.

One gram of the pure Ph_2CH-$SiHMe_2$ was placed in a two-necked round-bottom flask equipped with a side arm containing a filter frit and was dissolved in 25 mL of dry CCl_4. Freshly recrystallized NBS (1.6 g) was introduced, and the mixture was stirred for 30 min. The bromination occurred rapidly, with no radical initiator added. The reaction was complete after gentle reflux for 1 h. The succinimide was filtered off through the side arm of the reaction flask. After evaporation of the CCl_4, the viscous yellow residue isolated in 50% overall yield was shown to be pure by ^1H NMR. NMR: $\delta(^1H)$ 0.2 (6 H), 6.13 (6 H); 6.43 (d, 4 H); $\delta(^{13}C)$ 3.47 (CH_3), 66.1 (C-Br); 142.4 (i), 127.6 (o), 130.0 (m), 127.31 (p); $\delta(^{29}Si)$ 13.5.

$Ph_2BrSiSiBrPh_2$ (21).[30] NMR: $\delta(^{13}C)$ 134.8 (o), 127.9 (m), 130.4 (p), 132.2 (i); $\delta(^{29}Si)$ -4.4.

Attempted Preparation of Bridged Halonium Ions. Freshly sublimed $AlBr_3$ or triply distilled SbF_5 was used. A preweighed amount of SbF_5 or $AlBr_3$ dissolved (slurried in the case of $AlBr_3$) in 1 mL of dry SO_2ClF was treated with the appropriate amount of halide at -78 °C (using dry ice/acetone bath) in a dry 5-mm NMR tube under argon with vigorous stirring.

Acknowledgment. Support of our work by the National Science Foundation is acknowledged. We are grateful to Prof. W. Kutzelnigg and Dr. M. Schindler for providing a copy of their IGLO program. Prof. P. Boudjouk is thanked for providing silole samples.

Supplementary Material Available: Cartesian coordinates of the optimized structures of **1-9** (4 pages). Ordering information is given on any current masthead page.

Formation, Isomerization, and Cyclization Reactions of Hydroperoxyalkyl Radicals in Hexadecane Autoxidation at 160-190 °C

R. K. Jensen,* S. Korcek, and M. Zinbo

Contribution from Ford Motor Company, SRL-3083, P.O. Box 2053, Dearborn, Michigan 48121-2053. *Received January 21, 1992*

Abstract: Kinetic and mechanistic investigations of the effects of oxygen pressure on liquid-phase autoxidation reactions in hydrocarbons at elevated temperatures were carried out with hexadecane at 160-190 °C and at oxygen pressures from 4 to 120 kPa using a stirred-flow reactor. Results of studies of formation of primary oxidation products showed that the intramolecular α,γ and α,δ hydrogen abstraction reactions of peroxy radicals (reactions 4) are highly reversible and that the intermediate hydroperoxyalkyl radicals formed from these abstractions, besides addition of oxygen and reverse intramolecular hydrogen abstraction (isomerization) reactions (reactions -4) undergo cyclization reactions leading to formation of cyclic ether products (reaction 10). Kinetic analyses based on the proposed reaction scheme allowed derivation of the absolute rate constants for reactions 4, -4, and 10 of the intermediate α,γ- and α,δ-hydroperoxyhexadecyl radicals, HOOR*. The derived rate constants are in good agreement with published values from gas-phase oxidations.

Introduction

Investigations of the liquid-phase autoxidation of hexadecane with pure oxygen carried out in the stirred-flow microreactor at 100-110 kPa of O_2 and 120-180 °C led to the discoveries of α,γ and α,δ intramolecular hydrogen abstraction reactions of alkylperoxy radicals[1] and the cleavage reaction of α,γ-hydroperoxy-substituted ketones.[2] The occurrence of intramolecular hydrogen

(1) Jensen, R. K.; Korcek, S.; Mahoney, L. R.; Zinbo, M. *J. Am. Chem. Soc.* **1979**, *101*, 7574.

0002-7863/92/1514-7742$03.00/0

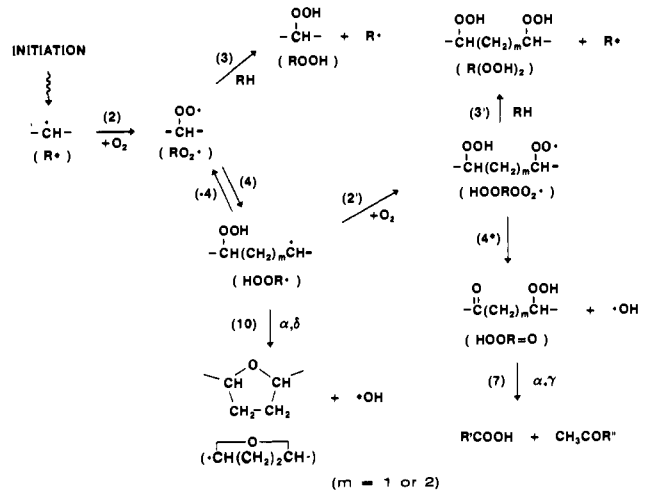

Figure 1. Reaction scheme for the autoxidation of hexadecane at elevated temperatures.

abstraction reactions explained the formation of difunctional oxidation products, namely α,γ- and α,δ-dihydroperoxides and hydroperoxy-substituted ketones, which together with monohydroperoxides are the major primary oxidation products at these reaction conditions.[1] The cleavage reaction of α,γ-hydroperoxy-substituted ketones was found to be one of the two independent processes of cleavage product formation.[2] It accounted for the formation of cleavage methyl ketones and 50–60% of alkanoic acids.

In the present study we describe the effects of oxygen pressure on kinetics and mechanisms of hexadecane autoxidation at elevated temperatures using a range of oxygen pressures from 4 to 120 kPa which includes atmospheric conditions. We then use the product analyses and a kinetic analysis to derive the absolute rate constants for intramolecular hydrogen abstraction (reaction 4; the reaction denotation system used throughout this work is consistent with that used in our previous publications[1,2]) as well as isomerization (reaction −4) and cyclization (reaction 10) of the intermediate α,γ- and α,δ-hydroperoxyhexadecyl radicals, HOOR• (see Figure 1 for the reaction scheme). Reactions −4 and 10 were previously documented by Benson.[3] The latter reaction is generally accepted as a source of cyclic ether products in the gas-phase oxidation of *n*-alkanes of carbon number 4 or greater in the temperature region 300–480 °C.[4] In the liquid phase the formation of cyclic ethers was detected in the oxidation of *n*-dodecane by air at 200 °C[5] and in the oxidation of substrates containing tertiary hydrogens, such as 2-methylhexadecane[6] and 2,4-dimethylpentane.[7]

Experimental Section

The reaction techniques, materials used and the analytical procedures for determination of hexadecane hydroperoxides, dihydroperoxides, ketones, hydroperoxy ketones, and scission ketones and acids were described previously.[1,2] The procedure for analysis of C_{16}-dialkyloxolanes has also been described previously.[8]

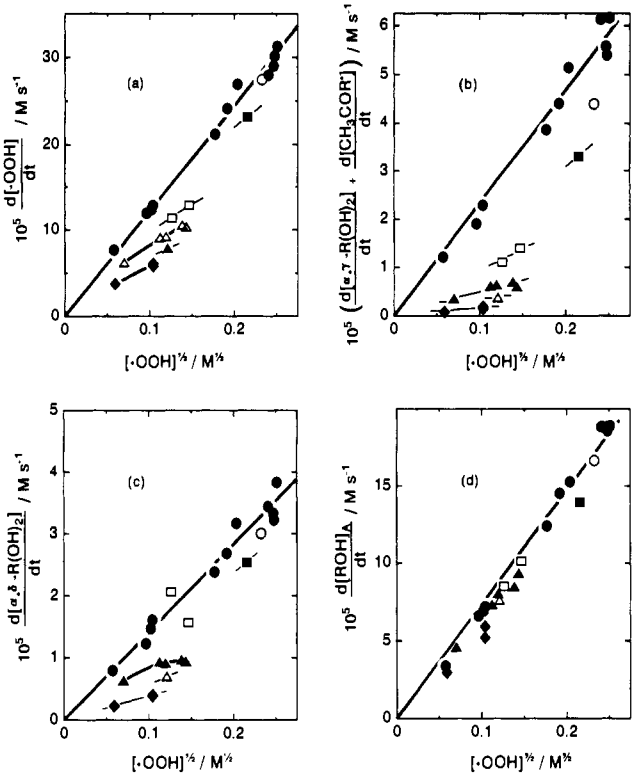

Figure 2. Rate of formation of hydroperoxides (a), difunctional products (b and c), and monofunctional products (d) vs $[-OOH]^{1/2}$ at 180 °C and at 5 (♦), 7 (△), 11–13 (▲), 19–20 (□), 34 (■), 57 (○), and 110–120 (●) kPa of oxygen.

Results and Discussion

Oxidation Products. Results of analyses of samples obtained from the autoxidation of hexadecane in a stirred-flow microreactor at 160–190 °C and 4–120 kPa of oxygen are summarized in Table I.

The C_{16} primary oxidation products include (1) isomeric hexadecyl hydroperoxides, ROOH, determined in sodium borohydride reduced oxidates (subscript A) as hexadecanols, $(ROH)_A$, (2) isomeric hexadecanediyl dihydroperoxides, $R(OOH)_2$, and hydroperoxyhexadecanones, HOOR=O, determined together as hexadecanediols, $(R(OH)_2)_A$, and (3) isomeric C_{16}-dialkyloxolanes, $-\overset{\frown O \frown}{CH(CH_2)_2CH}-$. Cleavage methyl ketones, CH_3COR', were determined as a series of 2-alcohols, $(CH_3CH(OH)R')_A$. Termination products, isomeric hexadecanones (R'COR''), were determined in triphenylphosphine reduced samples either directly or after derivatization.

Reaction Scheme. A reaction scheme which accounts for the results of hexadecane autoxidation at elevated temperatures obtained in this study and in our previous work[1,2] is given in Figure 1. According to this scheme, initiation of autoxidation occurs via the homolytic decomposition of peroxidic products (reaction 1). This reaction ultimately leads to formation of alkyl radicals, R•, which react with oxygen to produce alkylperoxy radicals, RO_2• (reaction 2). Alkylperoxy radicals either undergo irreversible intermolecular hydrogen abstraction (reaction 3), producing monohydroperoxide products, ROOH, or reversible intramolecular α,γ ($m = 1$) and α,δ ($m = 2$) hydrogen abstraction (reaction 4), leading to α,γ- and α,δ-hydroperoxy-substituted carbon radicals, HOOR•. These carbon radicals, depending on oxygen pressure, can either isomerize (reaction −4) or undergo intramolecular

(2) Jensen, R. K.; Korcek, S.; Mahoney, L. R.; Zinbo, M. *J. Am. Chem. Soc.* **1981**, *103*, 1742.
(3) Benson, S. W. *J. Am. Chem. Soc.* **1965**, *87*, 972. Symposium on the Mechanisms of Pyrolysis, Oxidation and Burning of Organic Materials, NBS Spec. Publ. No. 357, 1972, p 121. *Prog. Energy Combust. Sci.* **1981**, *7*, 125. *Oxidation Comm.* **1982**, *2*, 169.
(4) (a) Fish, A. In *Organic Peroxides*; Swern, D., Ed.; Wiley: New York, 1970; Vol. I, Chapter 3. (b) Fish, A. In *Oxidation of Organic Compounds*; Gould, R. F., Ed.; Advances in Chemistry Series; American Chemical Society: Washington, D.C., 1968; Vol. 76, p 69. (c) Berry, T.; Cullis, C. F.; Saeed, M.; Trimm, D. L. In *Oxidation of Organic Compounds*; Gould, R. F., Ed.; Advances in Chemistry Series; American Chemical Society: Washington, D.C., 1968; Vol. 76, p 86. (d) Barat, P.; Cullis, C. F.; Pollard, R. T. In *13th Int. Combustion Symposium*; The Combustion Institute; Pittsburgh, PA, 1977; p 179. (e) Walker, R. W. In *Reaction Kinetics*; Specialist Periodical Report; The Chemical Society: London, 1975; Vol. I, p 161. (f) Baldwin, R. R.; Bennett, J. P.; Walker, R. W. In *16th Int. Combustion Symposium*; The Combustion Institute: Pittsburgh, PA, 1977; p 1041. (g) Baldwin, R. R.; Bennett, J. P.; Walker, R. W. *J. Chem. Soc., Faraday Trans. 1* **1980**, *76*, 1075. (h) Baldwin, R. R.; Hisham, M. W. M.; Walker, R. W. *J. Chem. Soc., Faraday Trans. 1* **1982**, *78*, 1615.
(5) Boss, B. D.; Hazlett, R. N. *Can. J. Chem.* **1969**, *47*, 4175.
(6) Brown, D. M.; Fish, A. *Proc. R. Soc. London, Ser. A* **1969**, *308*, 547.
(7) Mill, T.; Montorsi, G. *Int. J. Chem. Kinet.* **1973**, *5*, 119.
(8) Zinbo, M.; Jensen, R. K. *Anal. Chem.* **1985**, *57*(1), 315.

Table I. Analysis of C_{16} Products from the Autoxidation of Hexadecane in the Stirred-Flow Microreactor

temp (°C)	P_{O_2} (kPa)	τ (s)	run	concentration (mM)									
				[–OOH]	[1-ROH]$_A$[a]	[2-ROH]$_A$[a]	[3--8-ROH]$_A$[a]	[ROH]$_A$[a]	[α,γ-R(OH)$_2$]$_A$[a]	[α,δ-R(OH)$_2$]$_A$[a]	[–CH(CH$_2$)$_2$CH–]	[4--8-R′COR″]$_C$[b,c]	[1--8-R′COR″]
160	4.66	340	245	3.56	0.08	0.52	2.49	3.09	0.11	0.39	0.046	0.018	
160	4.60	664	244	12.40	0.26	1.80	9.63	11.69	0.32	1.17	0.15	0.16	
160	5.85	475	275	7.42	0.20	1.03	5.11	6.34	0.144	0.72	0.088		
160	8.95	337	249	4.58	0.09	0.59	2.61	3.29	0.12	0.47	0.035	0.024	
160	8.81	653	248	17.38	0.34	2.16	10.54	13.04	0.40	1.80	0.13	0.2	
160	15.95	338	250	5.62	0.13	0.68	3.13	3.94	0.31	0.63	0.032	0.027	
160	15.86	655	251	22.62	0.53	3.03	13.57	17.13	1.01	2.66	0.13	0.25	
160	34.58	482	274	14.56	0.47	1.74	6.96	9.17	0.72	1.79	0.043		
160	65.66	485	273	16.72	0.56	1.69	6.83	9.08	0.89	1.85	0.063		
160	86.76	491	272	18.87	0.53	2.19	7.54	10.26	0.83	2.12	0.036		
160	109	397	269	13.28	0.52	1.53	5.95	8.00	0.89	1.51	0.05	0.057	
160	108	784	270	46.98	2.13	5.20	24.95	32.28	2.78	5.66	0.13	0.637	
170	9.71	204	284	6.38	0.14	0.84	4.30	5.28	0.144	0.688	0.078	0.03	
170	9.79	301	285	12.68	0.29	1.64	8.79	10.72	0.29	1.37	0.164	0.101	
170	19.9	204	286	8.63	0.24	1.06	4.80	6.10	0.38	0.96	0.061		
170	19.6	299	287	19.44	0.47	2.39	11.42	14.28	0.61	2.1	0.141	0.157	
170	58	204	288	11.99	0.38	1.44	5.78	7.60	0.61	1.33	0.036		
170	113	201	282	14.33	0.44	1.51	6.94	8.89	1.17	1.58	0.029	0.064	
170	111	297	283	28.94	0.82	2.9	13.91	17.63	1.96	3.17	0.054	0.232	
180	5	93	224	3.52	0.051	0.53	2.17	2.75	0.052	0.21		0.014	0.021
180	5	178	223	10.9	0.17	1.78	7.32	9.27	0.12	0.68		0.105	0.115
180	4.68	186	258	10.9	0.18	1.68	9.13	10.99	0.13	0.75	0.28	0.122	
180	7.34	186	259	14.7	0.27	2.23	11.68	14.18	0.23	1.30	0.30	0.158	
180	12.6	78	219	5.01	0.096	0.76	2.72	3.58	0.16	0.5	0.064	0.018	
180	12.2	138	218	12.9	0.21	1.96	7.94	10.11	0.37	1.29			
180	11.4	154	216	14.6	0.30	1.70	10.40	12.40	0.44	1.41	0.235	0.105	0.127
180	12.1	181	217	19.6	0.40	2.33	12.62	15.35	0.41	1.75	0.279	0.196	
180	11.3	198	215	20.5	0.43	2.67	15.44	18.54	0.34	1.87	0.39	0.219	0.274
180	20.2	140	225	15.9	0.49	1.78	9.65	11.92	0.48	2.88	0.20	0.12	0.153
180	19.25	167	260	22.1	0.51	2.56	13.87	16.94	0.94	2.63	0.231	0.239	
180	34.1	200	153	46.4	1.07	5.39	21.40	27.86	2.51	5.05		0.526	
180	46.4	200	277	47.8	1.2	5.62	22.20	29.02	1.58	5.27			
180	57.7	197	152	54.1	1.38	6.44	25.00	32.82	3.30	5.92		0.732	
180	80.2	205	276	72.1	1.89	7.93	28.93	38.75	2.81	7.29	0.145		
180	116	78	150	9.3	0.24	1.06	3.84	5.14	1.00	0.957		0.046	0.077
180	113	148	149	31.4	0.83	3.72	13.8	18.35	2.74	3.52		0.291	
180	116	202	151	63.1	1.75	6.91	29.50	38.16	3.46	7.73	0.138	0.98	1.93
190	4.99	69.3	262	5.17	0.09	0.72	4.56	5.37	0.070	0.32	0.171	0.045	
190	6.04	51.1	281	3.23	0.13	0.56	3.05	3.74	0.049	0.277	0.121		
190	7.71	68.7	265	6.65	0.14	0.98	5.64	6.76	0.15	0.57	0.191	0.056	
190	10.20	69.6	266	8.39	0.16	1.04	6.18	7.38	0.14	0.69	0.197	0.070	
190	15.45	69.2	263	10.79	0.22	1.40	7.04	8.66	0.25	1.13	0.202	0.072	
190	20.36	68.8	267	13.28	0.31	1.65	8.95	10.91	0.41	1.49	0.211	0.109	
190	51.7	51.0	280	14.87	0.41	1.53	6.56	8.50	0.83	1.59	0.078		
190	76.8	50.7	279	15.59	0.40	1.11	6.35	7.86	0.83	1.70	0.080	0.06	
190	102	50.7	278	18.01	0.69	2.46	6.16	9.31	0.93	1.69	0.054		
190	117	66.2	264	34.19	0.97	4.09	16.23	21.29	2.63	3.91	0.118	0.289	
190	120	50.0	271	20.56	0.63	2.09	9.66	12.38	1.58	2.64		0.111	

[a] Subscript A refers to concentrations determined in $NaBH_4$ reduced samples. [b] Subscript C refers to concentrations determined in Ph_3P reduced samples. [c] Hexadecanone isomers detectable as a separate group of products in Ph_3P reduced samples.

cyclization (α,δ only) (reaction 10) to produce C_{16} cyclic ethers, $-\overset{\overset{\text{O}}{\frown}}{\text{CH}(\text{CH}_2)_2\text{CH}}-$, and hydroxy radicals, or irreversibly react with oxygen to give hydroperoxy-substituted peroxy radicals, $HOOR'O_2^{\bullet}$ (reaction 2'). These hydroperoxyperoxy radicals, similarly as $RO_2^{\bullet}$, can undergo intermolecular hydrogen abstraction (reaction 3') to form dihydroperoxides, $R(OOH)_2$, and intramolecular abstraction of secondary hydrogen, similar to reaction 4, which leads to trifunctional oxidation products. In addition to reactions 2' and 4, $HOOR'O_2^{\bullet}$ undergoes an intramolecular abstraction reaction of tertiary hydrogen (reaction 4*) to form hydroperoxy-substituted ketone products, HOOR=O, and hydroxy radical. The α,γ-hydroperoxy ketone products undergo molecular decomposition to methyl ketones, CH_3COR', and alkanoic acids, R'COOH, via reaction 7.[9]

Formation of Primary C_{16} Products. Results of our present kinetic investigations and those reported previously[1,2] show that the rates of formation of hydroperoxides at a given hydroperoxide concentration decrease (1) with decreasing oxygen pressure (Figure 2a) and (2) with increasing temperature (e.g. at [–OOH] of 10 mM the rates at 160, 180, and 190 °C and 5 kPa are equal to ca. 87, 46, and 36% of the corresponding 110-kPa values). This decrease occurs mostly due to the decreased rate of formation of difunctional hydroperoxide products which is more pronounced with α,γ-substituted dihydroperoxides (Figure 2, b and c). The rate of formation of monohydroperoxide products (Figure 2d) is much less affected by reduced oxygen pressures. From all products analyzed, only the rate of formation of C_{16}-dialkyloxolanes increases with decreasing oxygen pressure (Figure 3). Results obtained at 160 and 190 °C are similar to those at 180 °C in Figure 2a–d.

The above kinetic information suggests that concentration of $HOOR'O_2^{\bullet}$ decreases with decreasing oxygen pressure more than that of $RO_2^{\bullet}$. Such preferential decrease must be due to the occurrence of reactions –4 and 10 which at lower oxygen pressures effectively compete for HOOR' with reaction 2'. No such competitive reactions, besides termination, consume R' which reacts with oxygen to give $RO_2^{\bullet}$ via reaction 2. On the basis of kinetic analysis for the scheme in Figure 1, the ratio of $[HOOR'O_2^{\bullet}]$ and $[RO_2^{\bullet}]$, ψ, is given by eq I

$$\psi = \frac{[\alpha,\gamma\text{-HOOR}'O_2^{\bullet}] + [\alpha,\delta\text{-HOOR}'O_2^{\bullet}]}{[RO_2^{\bullet}]} = \frac{k_{4\cdot\alpha,\gamma}}{k_3[RH] + k_{4^*\alpha,\gamma}} \frac{1}{1 + \dfrac{k_{-4\cdot\alpha,\gamma}}{k_{2'}[O_2]}} + \frac{k_{4\cdot\alpha,\delta}}{k_3[RH] + k_{4^*\alpha,\delta}} \frac{1}{1 + \dfrac{k_{-4\cdot\alpha,\delta} + k_{10\cdot\alpha,\delta}}{k_{2'}[O_2]}} \quad \text{(I)}$$

and the ratio of $[\alpha,\delta\text{-HOOR}^{\bullet}]$ to $[RO_2^{\bullet}]$, θ, by eq II.[10]

$$\theta = \frac{[\alpha,\delta\text{-HOOR}^{\bullet}]}{[RO_2^{\bullet}]} = \frac{k_{4\cdot\alpha,\delta}}{k_{-4\cdot\alpha,\delta} + k_{10\cdot\alpha,\delta} + k_{2'\cdot\alpha,\delta}[O_2]} \quad \text{(II)}$$

At high oxygen pressures, when $k_{2'}[O_2] \gg k_{-4} + k_{10}$, ψ approaches its maximum while θ approaches its minimum. At oxygen pressures within our experimental range (4–120 kPa) the values of ψ and θ depend on the relative values of $k_{2'}[O_2]$ and $k_{-4} + k_{10}$. It is clear, however, that with decreasing oxygen pressure ψ will decrease while θ will increase. This is consistent with the decreased rate of formation of difunctional hydroperoxide products and increased rate of formation of C_{16}-dialkyloxolanes at lower oxygen pressures, since these rates are proportional to $[HOOR'O_2^{\bullet}]$ and $[\alpha,\delta\text{-HOOR}^{\bullet}]$, respectively.

(9) See ref 2 for a detailed discussion of reaction 7.

(10) Derived using the steady-state approximation for each radical at sufficiently long kinetic chain length and assuming k_3 to be equal to $k_{3'}$ and terminations to occur via reactions 5b and 6 of $RO_2^{\bullet}$ and $HOOR'O_2^{\bullet}$.

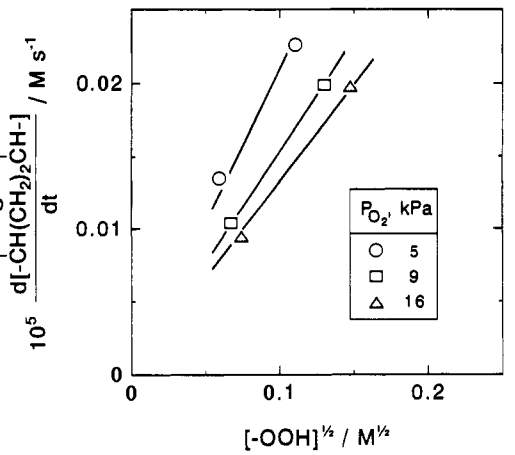

Figure 3. Rates of formation of dialkyloxolanes vs $[-OOH]^{1/2}$ at 180 °C and at different oxygen pressures.

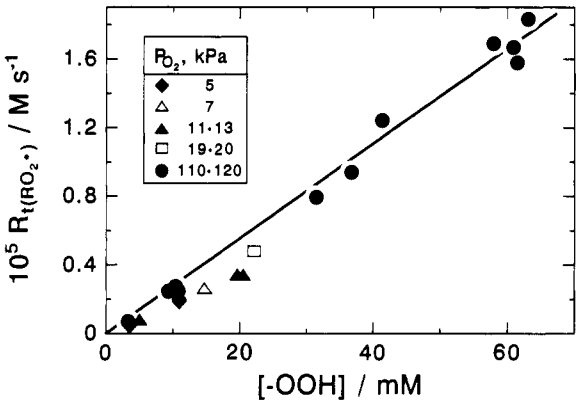

Figure 4. Rate of formation of peroxy radical termination products as a function of [–OOH].

Assuming that oxygen pressure is sufficiently high to transform all R' formed to $RO_2^{\bullet}$, the concentration of $RO_2^{\bullet}$ is given by eq III

$$[RO_2^{\bullet}] = \frac{(R_{RO_2\cdot})^{1/2}}{(2xk_5 + 2k_6)^{1/2}} \frac{1}{(1 + \psi)} \quad \text{(III)}$$

where $R_{RO_2\cdot}$ is the rate of formation of $RO_2^{\bullet}$, equal to the rate of initiation, R_i, and k_5 and k_6 are the rate constants for termination reactions.[1,2] Equation III suggests that $[RO_2^{\bullet}]$ approaches its minimum when $k_{2'}[O_2] \gg k_{-4} + k_{10}$, i.e., at high oxygen pressures. If $R_{RO_2\cdot}$ remains the same, $[RO_2^{\bullet}]$ should increase with decreasing oxygen pressure. Under such conditions, the rate of formation of monofunctional hydroperoxide products should also increase with decreasing oxygen pressure since the rate is proportional to $[RO_2^{\bullet}]$. However, no such increase has been observed; instead, some decrease at all temperatures occurred after reaching certain [–OOH]. The lower the oxygen pressure, the lower is [–OOH] at which decreases were observed. This finding suggests that at a given oxygen pressure there is a certain limiting [–OOH], i.e., limiting rate of initiation, at which the oxygen supply and concentration become insufficient to transform all R' to $RO_2^{\bullet}$ and that under such conditions alkyl radicals also contribute to termination. In such a case, $R_{RO_2\cdot}$ at low oxygen pressures must be lower than $R_{RO_2\cdot}$ at high oxygen pressures and lower than R_i. This view is supported by results shown in Figure 4 where the rates of initiation, determined from the rates of formation of termination products,[11] $R_{t(RO_2\cdot)}$, are plotted against [–OOH]. The lower values of $R_{t(RO_2\cdot)}$ at lower oxygen pressures confirm reduced contribution of $RO_2^{\bullet}$ and some contribution of R' to termination.

The increased concentration of R' may also be a contributing factor leading to the change of monohydroperoxide isomer dis-

(11) Jensen, R. K.; Korcek, S.; Zinbo, M.; Johnson, M. D. *Int. J. Chem. Kinet.* **1990**, *22*, 1095.

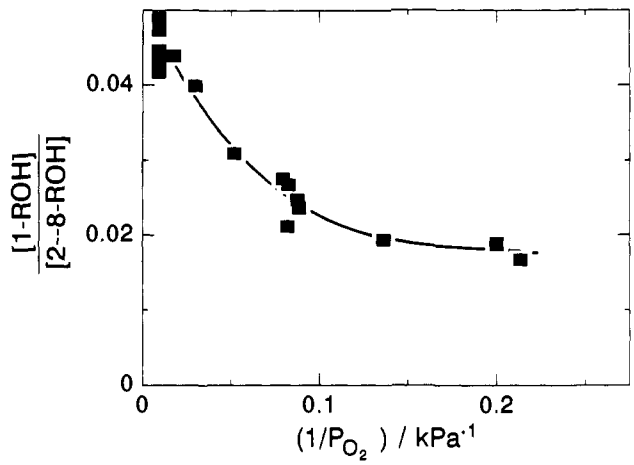

Figure 5. Ratio of rates of formation of primary and secondary monofunctional hydroperoxide products as a function of oxygen pressure.

tribution exhibited by decreased formation of primary 1-hexadecyl hydroperoxide at low oxygen pressures (Figure 5). This indicates lower concentration of primary $RO_2^{\bullet}$ at low oxygen pressures. It can be explained by the lower concentration of nonselective $^{\bullet}OH$ radicals due to their decreased rate of formation from reaction 4* and/or by higher concentration of secondary $R^{\bullet}$ and $RO_2^{\bullet}$. These higher concentrations would result from higher reactivity of primary versus secondary $R^{\bullet}$ in the radical transfer reaction with secondary hydrogens of RH. Consequently, the ratio of overall reactivity of primary versus secondary hydrogens in hydrogen abstraction reactions by mixtures of free radicals present in the autoxidized hexadecane at high oxygen pressures is found to be 1:5 while at oxygen pressures of 5 kPa it is 1:14.

At lower oxygen pressures the effects of the increased concentration of $R^{\bullet}$ and lower concentration of $RO_2^{\bullet}$ can be detected in the change in the isomer distribution and in the lower rate of formation of termination products due to cross-termination reactions. However, even at the lowest oxygen pressure the cross-termination reaction represents only a small fraction of the total termination and the predominant radical is $RO_2^{\bullet}$.

Kinetic Analysis. A kinetic analysis for the proposed reaction scheme (see Figure 1 and for a detailed scheme Figure 4 in ref 1) leads to the following expressions for the ratios of rates of product formation:[12]

$$\frac{\left(\frac{d[ROOH]}{dt}\right)_f}{\left(\frac{d[\alpha,\gamma\text{-R(OOH)}_2]}{dt}\right)_f + \left(\frac{d[\alpha,\gamma\text{-HOOR=O}]}{dt}\right)_f} = \frac{k_3[RH]}{k_3[RH] + k_{4^{\bullet}\alpha,\gamma}} \frac{[RO_2^{\bullet}]}{[\alpha,\gamma\text{-HOORO}_2^{\bullet}]} = \frac{k_3[RH]}{k_{4\cdot\alpha,\gamma}}\left(1 + \frac{k_{-4\cdot\alpha,\gamma}}{k_{2'\cdot\alpha,\gamma}[O_2]}\right) \quad \text{(IV)}$$

$$\frac{\left(\frac{d[ROOH]}{dt}\right)_f}{\left(\frac{d[\alpha,\delta\text{-R(OOH)}_2]}{dt}\right)_f + \left(\frac{d[\alpha,\delta\text{-HOOR=O}]}{dt}\right)_f} = \frac{k_3[RH]}{k_3[RH] + k_{4^{\bullet}\alpha,\delta}} \frac{[RO_2^{\bullet}]}{[\alpha,\delta\text{-HOORO}_2^{\bullet}]} = \frac{k_3[RH]}{k_{4\cdot\alpha,\delta}}\left(1 + \frac{k_{-4\cdot\alpha,\delta} + k_{10\cdot\alpha,\delta}}{k_{2'\cdot\alpha,\delta}[O_2]}\right) \quad \text{(V)}$$

$$\frac{\left(\frac{d[-CH(CH_2)_2CH-]}{dt}\right)_f}{\left(\frac{d[\alpha,\delta\text{-R(OOH)}_2]}{dt}\right)_f + \left(\frac{d[\alpha,\delta\text{-HOOR=O}]}{dt}\right)_f} = \frac{k_{10\cdot\alpha,\delta}}{k_3[RH] + k_{4^{\bullet}\alpha,\delta}} \frac{[\alpha,\delta\text{-HOOR}^{\bullet}]}{[\alpha,\delta\text{-HOORO}_2^{\bullet}]} = \frac{k_{10\cdot\alpha,\delta}}{k_{2'\cdot\alpha,\delta}[O_2]} \quad \text{(VI)}$$

The ratios of rates can be obtained from the stirred-flow-reactor experiments as the ratios of the corresponding concentrations in the reactor[1] or as the ratios of the yields of corresponding products obtained from the $NaBH_4$ and Ph_3P reductions of oxidates.[13,14] Thus,

$$\frac{([ROH]_A)_\tau}{([\alpha,\gamma\text{-R(OH)}_2]_A)_\tau + ([CH_3CH(OH)R']_A)_\tau} = \frac{k_3[RH]}{k_{4\cdot\alpha,\gamma}}\left(1 + \frac{k_{-4\cdot\alpha,\gamma}}{k_{2'\cdot\alpha,\gamma}[O_2]}\right) \quad \text{(VII)}$$

$$\frac{([ROH]_A)_\tau}{([\alpha,\delta\text{-R(OH)}_2]_A)_\tau} = \frac{k_3[RH]}{k_{4\cdot\alpha,\delta}}\left(1 + \frac{k_{-4\cdot\alpha,\delta} + k_{10\cdot\alpha,\delta}}{k_{2'\cdot\alpha,\delta}[O_2]}\right) \quad \text{(VIII)}$$

$$\frac{([-CH(CH_2)_2CH-]_A)_\tau}{([\alpha,\delta\text{-R(OH)}_2]_A)_\tau} = \frac{k_{10\cdot\alpha,\delta}}{k_{2'\cdot\alpha,\delta}[O_2]} \quad \text{(IX)}$$

Equations VII–IX can be used in the determination of rate constants from the ratios of product concentrations obtained from the stirred-flow-reactor experiments as a function of oxygen concentration.

Oxygen Concentration. Oxygen solubility in hexadecane was calculated using parameters previously determined experimentally in our laboratory at temperatures from 24 to 190 °C.[15]

Rate Constants. Plots of experimental data consistent with eqs VII–IX are given in Figure 6. The composite rate constants derived from the slopes and intercepts of these plots, $k_3[RH]/k_4$, $(k_{-4} + k_{10})/k_{2'}$, and $k_{10}/k_{2'}$, are given in Table II. The individual absolute rate constants calculated from the above composite rate constants are also given in Table II. Values of k_4 were obtained from ratios $k_3[RH]/k_4$ using values of k_3 determined previously.[16] Values of k_{-4} and k_{10} were obtained assuming a diffusion-controlled value of 10^9 M^{-1} s^{-1} for $k_{2'}$. The absolute rate constants on a per hydrogen basis were calculated using the number of available hydrogens in reactions 4-α,γ, 4-α,δ, −4-α,γ, and −4-α,δ equal to 3.17, 2.94, 1, and 1, respectively.

Discussion of Results. Values of absolute rate constants for reactions 4, −4, and 10 involving formation, isomerization, and cyclization of secondary hydroperoxyalkyl radicals reported in this work represent the first experimentally determined values of these constants obtained in the liquid phase.

(12) Derived using the steady-state approximation for each radical at sufficiently long kinetic chain length and assuming k_3 to be equal to k_3, and terminations via reactions of $RO_2^{\bullet}$ and $HOORO_2^{\bullet}$.

(13) It was previously reported in ref 1 that at sufficiently long kinetic chain length

$$[ROOH] \approx [ROH]_A$$

$$[R(OOH)_2] \approx [R(OH)_2]_C$$

$$[HOOR{=}O] \approx [R(OH)_2]_A - [R(OH)_2]_C$$

$$[R(OOH)_2] + [HOOR{=}O] \approx [R(OH)_2]_A$$

$$[CH_3COR'] \approx [CH_3CH(OH)R']_A$$

where the subscript letter in concentration terms designates the reducing agent used; A corresponds to $NaBH_4$ and C to Ph_3P.

(14) $[CH_3CH(OH)R']_A$ represents that portion of α,γ-HOOR=O which was decomposed via reaction 7 to give CH_3COR'.[2]

(15) Jensen, R. K.; Korcek, S.; Zinbo, M. *Oxidation Commun.* **1974**, *13*(4), 258.

(16) Jensen, R. K.; Johnson, M. D.; Korcek, S.; Zinbo, M. Unpublished data.

(17) Reference 2. Supplementary material.

Table II. Rate Constants

rate constant	α, γ				α, δ			
	160 °C	170 °C	180 °C	190 °C	160 °C	170 °C	180 °C	190 °C
$(k_3[RH]/k_4)(k_{-4} + k_{10})/k_{2'}$ (mM)[a]	2.0	2.5	3.3	4.2	0.52	0.59	1.10	1.38
$k_3[RH]/k_4$[b,c]	3.2	2.8	1.5	1.8	5.0	5.4	4.7	4.4
$k_{10}/k_{2'}$ (mM)[d]					0.0165	0.0297	0.0428	0.0628
$(k_4 + k_{10})/k_{2'}$ (mM)	0.6	0.9	2.2	2.3	0.11	0.11	0.24	0.32
k_4 (s^{-1})	84	150	450	610	54	78	140	260
k_4/H (s^{-1})	26	48	140	190	18	27	48	87
k_{-4} (s^{-1})	6×10^5	9×10^5	2.2×10^6	2.3×10^6	1.1×10^5	1.1×10^5	2.4×10^5	3.2×10^5
k_{10} (s^{-1})					1.65×10^4	2.97×10^4	4.28×10^4	6.28×10^4

[a] Errors in values of slopes obtained from linear regression curves shown in Figure 6 are ±(0.1, 0.2, 0.1, 0.1) for α,γ and ±(0.06, 0.04, 0.04, 0.05) for α,δ at 160, 170, 180, and 190 °C, respectively. [b] Errors in values of intercepts obtained from linear regression curves shown in Figure 6 are ±(0.3, 0.4, 0.3, 0.6) for α,γ and ±(0.3, 0.1, 0.2, 0.2) for α,δ at 160, 170, 180, and 190 °C, respectively. [c] Reported values differ from those in ref 2. In the latter case they were obtained from measurements at oxygen pressure of 110–120 kPa only. [d] Errors in values of slopes obtained from linear regression curves shown in Figure 6 are ±0.0001 at all temperatures.

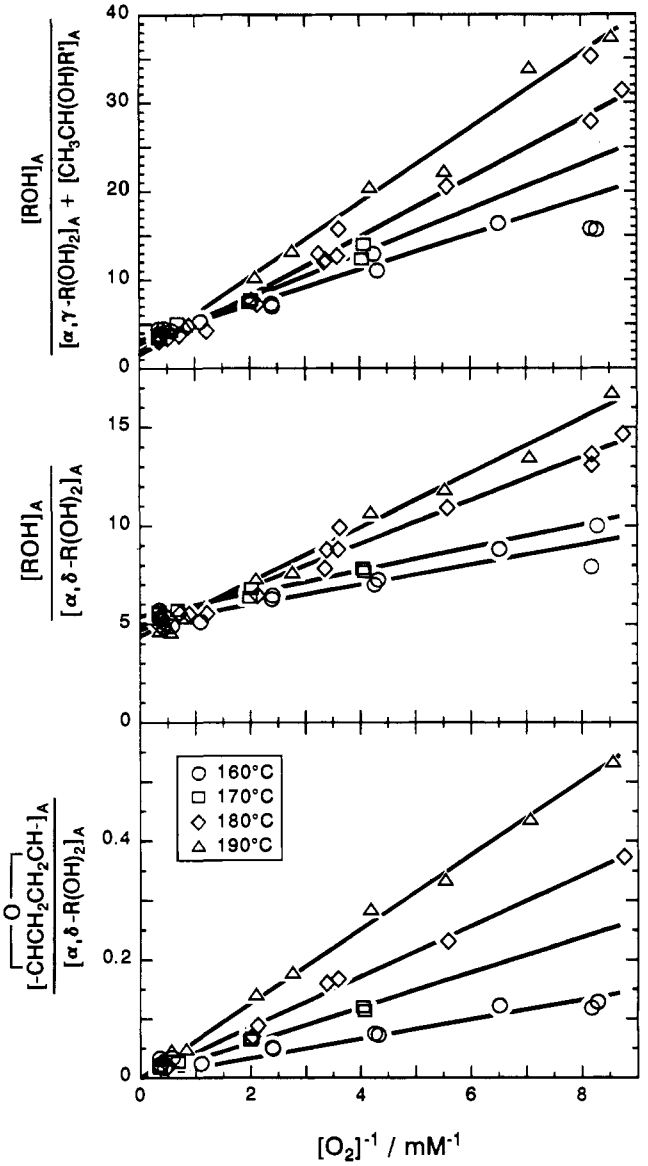

Figure 6. Plots of experimental data consistent with eqs VII–IX.

Relevant data were reported by Baldwin et al.[4] for intramolecular abstraction of secondary hydrogen by 2-pentylperoxy (α,γ abstraction) and *n*-pentylperoxy (α,δ abstraction) radicals in the gas phase. Plots of their gas-phase data at 480 °C along with our liquid-phase data at 160–190 °C shown in Figure 7 yielded the Arrhenius parameters for reactions 4-α,γ and 4-α,δ listed in Table III. The activation energy for α,γ abstraction which involves a six-membered-ring transition state is about the same as that of intermolecular abstraction as would be expected. The

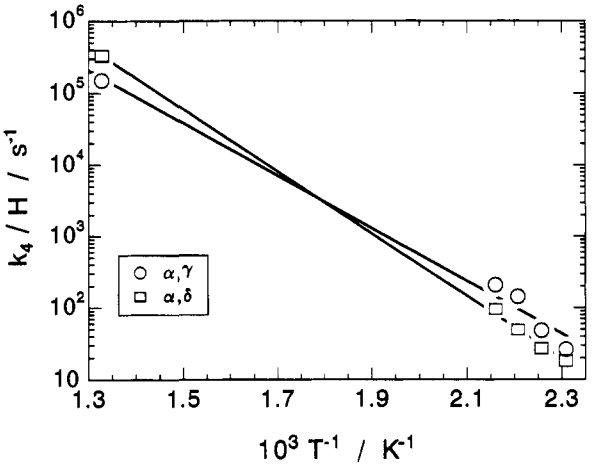

Figure 7. Plot of the rate of intramolecular hydrogen abstraction as a function of temperature.

Table III. Arrhenius Parameters

rate constant	log A/H (s^{-1})	E_a (kcal mol^{-1})
$k_{4\text{-}\alpha,\gamma}$/H[a]	10.1	17
$k_{4\text{-}\alpha,\delta}$/H[a]	11.3	20.0
$k_{-4\text{-}\alpha,\gamma}$/H[b]	11.9	12
$k_{-4\text{-}\alpha,\beta}$/H[b]	12.5	15.0
$k_{10\text{-}\alpha,\delta}$/H[c]	12.7	16.7

[a] Errors in log A/H and E_a estimated from linear regression analysis of the Arrhenius plots (assuming no error in gas-phase values for k_4 at 480 (°C) are ±0.5 s^{-1} and ±1 kcal mol^{-1} for $k_{4\text{-}\alpha,\gamma}$ and ±0.1 s^{-1} and ±0.2 kcal mol^{-1} for $k_{4\text{-}\alpha,\delta}$. [b] Values of E_a are estimated from the values for k_4 based on the difference in bond energy between ROOH and secondary RH which is equal to 5 kcal.[3] Values for log A/H were obtained from our experimental data using the estimated E_a. [c] Errors in log A/H and E_a estimated from the Arrhenius plots for $k_{10\text{-}\alpha,\delta}$ are ±0.7 s^{-1} and ±1.0 kcal mol^{-1}.

activation energy for α,δ abstraction involving a seven-membered ring is higher, but the 3-kcal/mol difference is less than the ring-strain difference which should be about 7 kcal/mol.[3] The A factors for these reactions would be expected to be about 10^{11}, which is the value found for α,δ abstraction. The A factor of 10^{10} for α,γ is probably too low. This could be due to the uncertainty in determination of α,γ reaction products which include a series of lower carbon number methyl ketones from decomposition of α,γ-hydroperoxy ketones.

The data for isomerization of the hydroperoxyalkyl radicals, reaction −4, are certainly less precise than those for reaction 4 since they are based on the ratios of slopes to intercepts from the plots. Moreover, no relevant data are available from the literature for comparison. However, it is reasonable to assume that the enthalpy change in reactions 4 and −4 is equivalent to the bond energy difference between ROOH and secondary RH which should be about 5 kcal.[3] This assumption is the basis for the Arrhenius parameters reported in Table III for reaction −4.

Rate constants for cyclization reactions of α,δ-hydroperoxyalkyl radicals (reaction 10) obtained in this study cannot be compared to other results since no information has been reported for either the gas or the liquid phase. However, relevant literature data are available for cyclization reactions of α,γ-hydroperoxyalkyl radicals in the gas phase. Using the data of Bastow and Cullis[18] at 250–315 °C and Knox and Kinnear[19] at 250–400 °C for the ratio of rates of formation of 2,4-dimethyloxetane to acetone in the combustion of *n*-pentane gives $k_{10\text{-}\alpha,\gamma} = 10^{12}\exp(-17.5/RT)\ s^{-1}$. From this equation it is possible to calculate the rate constant for cyclization of α,γ-hydroperoxyalkyl radicals for our temperature range as equal to $1.5\text{–}5.5 \times 10^3\ s^{-1}$. Comparing these estimated values to the rates of competing reactions 2′ and −4 predicts that concentrations of disubstituted oxetanes produced by reaction 10-α,γ would be less than 10^{-5} M under our conditions. These values are below the detection limits of our analytical procedures. Mill[20] reported Arrhenius parameters for α,γ cyclization of a tertiary radical from oxidation of 2,4-dimethylpentane in the liquid phase at 100 °C. The activation energy in that case was 3.5 kcal/mol less than that estimated from the gas-phase data for secondary radicals.

(18) Bastow, A. W.; Cullis, C. F. *Proc. R. Soc. London, A* **1974**, *341*, 195.
(19) Knox, J. H.; Kinnear, C. G. In *13th Int. Combustion Symposium*; The Combustion Institute: Pittsburgh, PA, 1977; p 217.
(20) Mill, T. In *13th Int. Combustion Symposium*; The Combustion Institute: Pittsburgh, PA, 1971; p 237.

Solvophobic and Entropic Driving Forces for Forming Velcraplexes, Which Are Four-Fold, Lock-Key Dimers in Organic Media[1,2]

Donald J. Cram,* Heung-Jin Choi, Judi A. Bryant, and Carolyn B. Knobler

Contribution from the Department of Chemistry and Biochemistry, University of California, Los Angeles, Los Angeles, California 90024. *Received March 2, 1992*

Abstract: Systems have been prepared composed of aromatic groups rigidly arranged to form ~15 by ~20 Å rectangular surfaces containing two regularly spaced protruding methyls at 3 and 9 o'clock and two methyl-sized holes at 12 and 6 o'clock (e.g., **1**). These molecules form dimers with large common surfaces in which the four methyl groups insert into the four holes. The resulting complexes have 82 to 132 intermolecular atom-to-atom contacts at van der Waals distances +0.2 Å (five crystal structures). Substitution of ethyls or hydrogens for the central aryl methyls eliminates complexation. Eight substituents attached at the periphery of the monomers extend the surfaces and profoundly affect the binding free energies ($-\Delta G°$ values) of the complexes, which range from <1 to >9 kcal mol^{-1} in $CDCl_3$ at temperatures −30 to 25 °C. Peripheral substituents with rotational degrees of freedom inhibit homodimerization. Activation free energies ($\Delta G^{\ddagger}$) for five dimerizations ranged from 8 to 10 kcal mol^{-1} and for five dissociations from 10 to 15 kcal mol^{-1} (in $CDCl_3$), suggesting their transition states to be very poorly solvated. The $-\Delta G°$ values for dimerization with notable exceptions increased dramatically with solvent polarity and polarizability. Enthalpies (ΔH values) ranged from +6 to −8 kcal mol^{-1} and entropies (ΔS values) from −6 to +40 cal mol^{-1} K^{-1}. Some dimerizations were entropy driven and enthalpy opposed, pointing to large solvophobic effects in organic media.

This paper reports the results of a study of complexation between two molecules, each of which possesses both host and guest character.[3] The complexing partners are highly preorganized[4] for complexation in such a way that each possesses a large rectangular face approximately 15 by 20 Å containing two protruding "up" methyls at 3 and 9 o'clock and two methyl-sized cavities at 12 and 6 o'clock lined by a sloping aryl face, an "out" methyl, and two oxygens. Prototypical structure **1a**, when rotated 90° about an axis normal to the page, gives view **1b**, which when turned over and placed on top of **1a**, beautifully forms a complex containing a large surface common to each partner, locked together by four methyl groups fitting into four cavities. In CPK models of the complex **1·1**, the monomers can neither slip nor rotate with respect to one another because of the four methyl locks. The dimerization is illustrated by A + B → C in the simplified drawings. In models of **1·1**, four sets of the quinoxaline "wings" contact one another, with their inner six-membered rings lying face-to-face.

All of the systems of this paper contain four conformationally mobile pentyl groups located on the side of each monomer opposite the complexing face. These "feet" provide monomer and dimer with the solubility in organic solvents required for this study. Models of **1·1** suggest to the viewer a globular jelly fish containing eight tentacles. Complexing systems **1** and **4–18** are further characterized by the absence in their structures of hydrogen bonds, ion pairs, or metal ligation sites common to many stable complexes. This leaves dipole–dipole, van der Waals, and solvophobic attractions as driving forces for complexation.

An earlier paper reported the synthesis of quinoxaline dimer **1·1** and quinoxaline monomers **2** and **3** as well as pyrazine dimer **4**.[5] Noncomplexing compound **3** is conformationally mobile, existing in a vase (C_{4v}) conformation (**3a**) at 25° and above, and in a kite (C_{2v}) conformation (**3b**) similar to that of **1a** at temperatures below −50 °C. The arylmethyls of **1** and arylethyls of **2** sterically inhibit formation of the vase conformations but undergo

(1) Host–Guest Complexation. 62.
(2) We warmly thank the U.S. Public Health Service for supporting Grant GE-12640.
(3) Two communications have appeared which collectively describe a small fraction of the work reported here: (a) Bryant, J. A.; Knobler, C. B.; Cram, D. J. *J. Am. Chem. Soc.* **1990**, *112*, 1254. (b) Bryant, J. A.; Ericson, J. L.; Cram, D. J. *J. Am. Chem. Soc.* **1990**, *112*, 1255.
(4) Cram, D. J. *Angew. Chem. Int. Engl. Ed.* **1986**, *25*, 1039–1057.
(5) Moran, J. R.; Ericson, J. L.; Dalcanale, E.; Bryant, J. A.; Knobler, C. B.; Cram, D. J. *J. Am. Chem. Soc.* **1991**, *113*, 5707–5714.

0002-7863/92/1514-7748$03.00/0